Laser magnetic resonance spectrum of HCO on the D_2O 108 μ laser line

Joel M. Cook

Chemistry Department, Rice University, Houston, Texas 77001

K. M. Evenson

Quantum Electronics Division, National Bureau of Standards, Boulder, Colorado 80302

Carleton J. Howard

Aeronomy Laboratory, NOAA Environmental, Research Laboratories, Boulder, Colorado 80302

R. F. Curl, Jr.

Chemistry Department, Rice University, Houston, Texas 77001
(Received 22 September 1975)

An LMR spectrum on the 108 μ D_2O laser line has been observed and assigned to the $8_{2,6}$—$7_{1,7}$ rotational transition of HCO. The spectra of both π (parallel) and σ (perpendicular) polarizations have been fitted by the least squares method, giving excellent agreement between the calculated and observed magnetic fields. The rotational frequency obtained from the fittings has been used to determine the A rotational constant. In addition, the electron spin-rotational splitting of each rotational level and the Fermi constant have been determined.

INTRODUCTION

Laser Magnetic Resonance (LMR) is a very sensitive technique for the observation of paramegnetic species which exist in the gas phase. Both stable and transient paramagnetic species can be and have been observed. Molecules which have been studied are O_2,[1] NO_2,[2] NO,[3] OH,[4] CH,[5] HO_2,[6] and NH_2.[7]

A description of the LMR technique parallels very closely that of conventional, gas phase ESR. In the LMR experiment a laser operating in the far infrared replaces the microwave radiation source of ESR. Zeeman components of various hyperfine sublevels of a pure rotational transition are brought into coincidence with the laser radiation by means of Zeeman tuning with an external magnetic field. The resulting absorption of laser radiation produces a signal which appears as the first derivative of the absorption line if the magnetic field is modulated with an amplitude which is much less than the linewidth of the transition.

The LMR method is quite sensitive compared with other forms of magnetic resonance—indeed, compared with many forms of spectroscopy.[8] This enhanced sensitivity over other forms of magnetic resonance results principally from operating at a much higher frequency and from the fact that the absorbing medium is within the laser cavity.

Because of its great sensitivity and its ability to detect paramagnetic species directly, LMR is a very useful technique for the study of free radical reactions in the gas phase.[8] Alternatively, a large amount of information of purely spectroscopic nature can be derived from the detailed analysis of LMR spectra. Information concerned with the various hyperfine interactions, Zeeman interactions, and the rotational Hamiltonian can be so obtained. This, in turn, leads to a better understanding of the geometry and electronic structure of the species. It is this spectroscopic facet of LMR with which we are here concerned.

This work reports the observation of the Zeeman components of a rotational transition of HCO using the 2.783 THz D_2O laser line, the assignment of these transitions to the $8_{2,6} - 7_{1,7}$ rotational transition, and the fitting of this spectrum with the parameters of a hyperfine Hamiltonian.

HCO has been the subject of several previous spectroscopic investigations. The red bands have been studied by Herzberg and Ramsay,[9] by Johns, Priddle and Ramsay,[10] and more recently by Brown and Ramsay.[11] The solid state ESR has been studied by Adrian *et al.*[12] and by Holmberg.[13] The a-type R branch rotational lines have been studied with the gas phase ESR technique by Bowater, Brown, and Carrington,[14] Austin, Levy, Gottlieb, and Radford,[15] and Boland, Brown, and Carrington.[16] The a-type $1_{0,1} - 0_{0,0}$ transition has been observed by Saito.[17] This work reports the first LMR study of this molecule and the first observation of a b-type rotational transition.

EXPERIMENTAL

The HCO free radicals were produced by reacting atomic fluorine with formaldehyde

$$F + H_2CO \rightarrow HF + HCO.$$

The F atoms are produced by an electric discharge in CF_4. Special analyzed He in a $\frac{10}{1}$ He/CF_4 ratio was used to stabilize the discharge. The H_2CO was produced by heating solid USP paraformaldehyde.

The sample mixture is continuously pumped through a portion of the cavity of a D_2O laser operating at 2.783 THz. A magnetic field surrounding the sample area is then used to bring the Zeeman components into coincidence with the laser. A Brewster angle diaphragm sep-

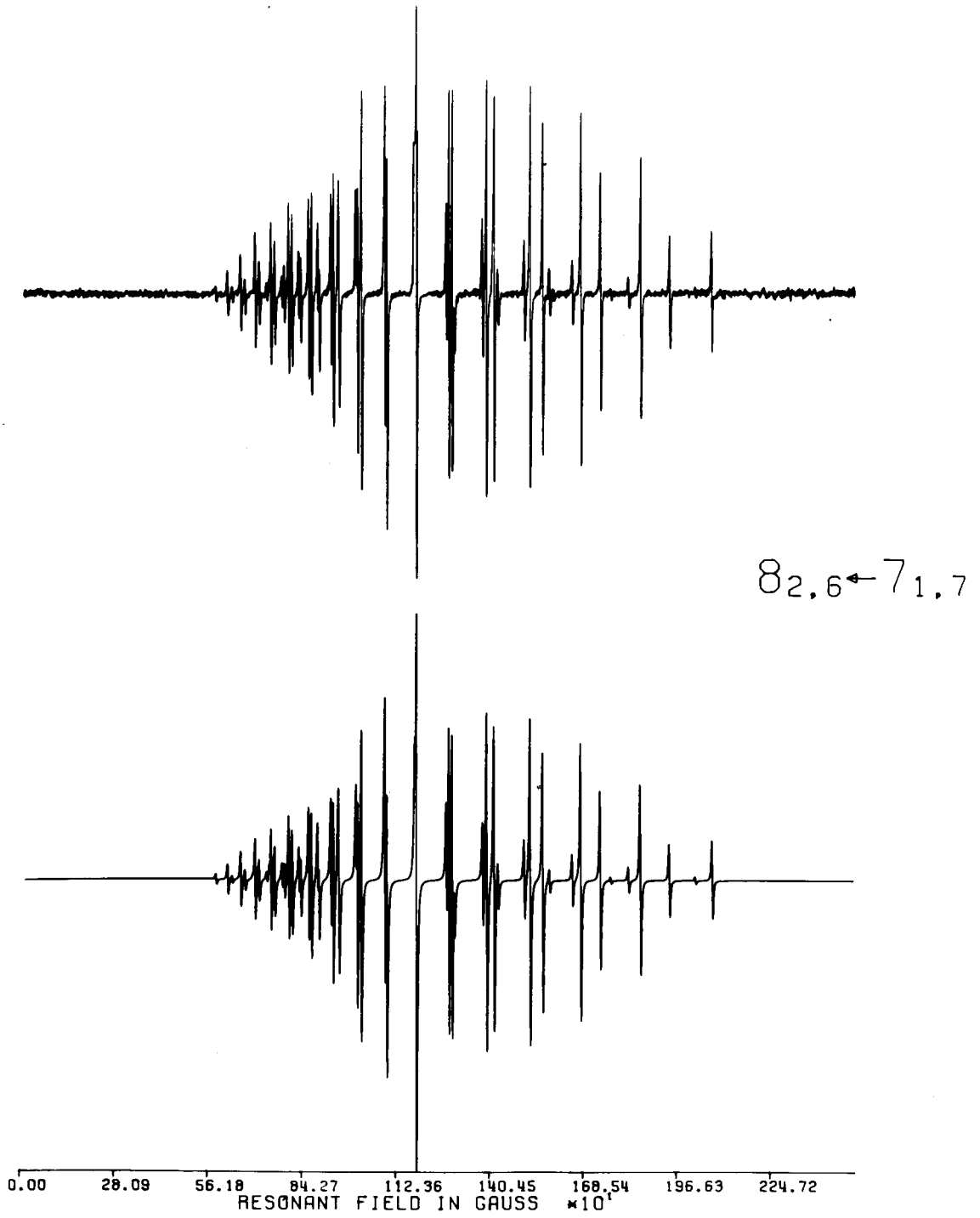

FIG. 1. These traces are the observed and calculated π polarization spectra. The upper trace is the observed and the lower the synthesized from the parameters obtained by least-square fitting.

arates the sample region from the gas laser. This allows the laser radiation to be polarized either parallel to the external magnetic field or perpendicular to it. In addition, the diaphragm serves to reflect a small amount of the laser radiation out into a liquid–helium cooled bolometer detector. A diagram of the spectrometer can be found in Ref. 2.

The laser frequency can be shifted by a few MHz from the central frequency by slightly altering the cavity length. This allows a determination of whether the Zeeman sublevels involved in the absorptions are approaching each other or diverging as the magnetic field is increased.

OBSERVATIONS

The spectrum observed by LMR depends on the orientation of the polarization of the laser radiation relative to the applied magnetic field. If the electric field of the laser radiation is parallel to the external field (π polarization), the selection rule is $\Delta M_F = 0$, while if the two

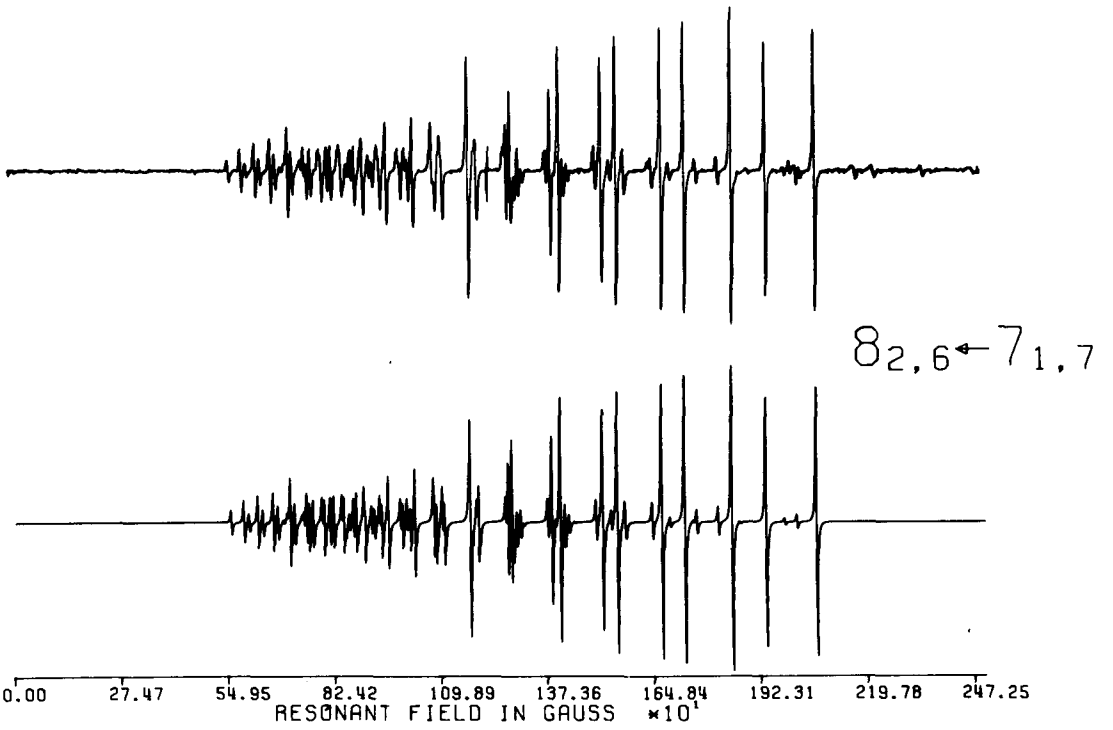

FIG. 2. The traces also show the observed and calculated spectra, this time for σ polarization. The upper is observed, the lower is synthesized from the parameters obtained by least-square fitting.

fields are perpendicular (σ polarization), the selection rules are $\Delta M_F = \pm 1$. Here M_F is the projection of the total angular momentum on the magnetic field direction.

The observed spectra of both polarizations are shown in Figs. 1 and 2. The observed lines were measured to 0.5 G excepting lines which occurred below 600 G and these measurements are tabulated in Table I. (The gaussmeter used did not operate below 600 G.)

It is possible to shift the laser frequency slightly by changing the cavity length as was mentioned above. In all cases, the lines are seen to move to higher field as the laser frequency increases. This indicates that the transitions involved must originate in the $M_S = -\frac{1}{2}$ level of the lower rotational level and must terminate in the $M_S = +\frac{1}{2}$ levels of the upper rotational level and that the rotational frequency is less than the laser frequency. Any other combination of levels would produce lines which tuned the wrong direction or scarcely at all.

THEORY

The Hamiltonian for a paramagnetic asymmetric rotor containing one nuclear spin in a magnetic field has been described by several authors.[2,14,18–20] HCO itself has one unpaired electron and one nuclear spin of $\frac{1}{2}$.

We chose to set up the calculation of the various energy levels in an "uncoupled" basis, i.e., $|N_{K-K+} M_N S M_S I M_I\rangle$, where the various M's represent the projections of the rotational, electron spin and nuclear spin, angular momenta on the field-defined z axis. We chose this basis primarily because of ease and speed of computation. The basis set (or coupling scheme) used in no way affects the results as the levels are obtained by setting up and diagonalizing a Hamiltonian matrix.

In choosing an appropriate Hamiltonian for this specific system, it seems advisable to first write down a fairly complete Hamiltonian and then treat those portions of that Hamiltonian which are of a size complementary to the accuracy of the observed data.

The fairly complete Hamiltonian which we began with is

$$\hat{H}_{\mathrm{TOT}} = \hat{H}_{\mathrm{ROT}} + \hat{H}_{\mathrm{HYP}} + \hat{H}_Z. \tag{1}$$

The terms on the right hand side of Eq. (1) take into account the rotational, the hyperfine and fine, and the Zeeman interactions, respectively. Let us now examine each of these in turn.

The rotational Hamiltonian includes the rigid rotor and centrifugal distortion effects. Since we are at present concerned with a single rotational transition, we just introduce a parameter corresponding to the rotational frequency.

$$\hat{H}_{\mathrm{HYP}} = \epsilon_{aa}\hat{N}_a\hat{S}_a + \epsilon_{bb}\hat{N}_b\hat{S}_b + \epsilon_{cc}\hat{N}_c\hat{S}_c + (aa)_I\hat{I}_a\hat{S}_a + (bb)_I\hat{I}_b\hat{S}_b + (cc)_I\hat{I}_c\hat{S}_c + (0)_I\hat{I}\cdot\hat{S}, \tag{2}$$

where $(aa)_I + (bb)_I + (cc)_I = 0$. The fine and hyperfine Hamiltonian consists of three parts: the molecular rotation–electron spin interaction, the magnetic dipole–dipole interaction between the proton and the electron, and the Fermi contact interaction. Two of the three spin–rotation parameters can be determined as can be the Fermi contact constant $(0)_I$, and were thus used in fitting the spectrum. The dipole–dipole constants were taken from the analysis of Boland[16]

TABLE I. Observed lines and assignments. Lines used in fitting have obs–calc reported.

obs[a]	M_F'	Index′	M_F	Index	obs–calc[a]
			π polarization		
620.2	6	4	6	1	0.1
633.9	7	3	7	2	
659.7	5	4	5	1	0.5
672.7	6	4	6	2	0.5
703.0	4	4	4	1	0.5
714.8	5	4	5	2	0.2
737.5	5	3	5	1	−0.2
744.7	6	3	6	2	−0.3
750.4	3	4	3	1	0.0
761.8	4	4	4	2	0.2
783.5	4	3	4	1	−0.1
790.1	5	3	5	2	0.0
803.6	2	4	2	1	0.0
813.8	3	4	3	2	0.2
834.9	3	3	3	1	0.8
839.4	4	3	4	2	−0.2
863.1	1	4	1	1	0.0
871.8	2	4	2	2	0.1
889.8	2	3	2	1	−0.3
894.4	3	3	3	2	0.1
929.9	0	4	0	1	−0.1
936.9	1	4	1	2	0.1
953.3	1,2	3,3	1,2	1,2	
1005.1	−1	4	−1	1	−0.2
1010.2	0	4	0	2	0.3
1021.8	0,1	3,3	0,1	1,2	
1092.4	−2,−1	4,4	−2,−1	1,2	
1098.4	−1,0	3,3	−1,0	1,2	
1186.9	−3,−2,−2,−1	4,4,3,3	−3,−2,−2,−1	1,2,1,2	
1277.8	−2	3	−2	2	0.2
1285.2	−3	3	−3	1	0.0
1295.3	−3	4	−3	2	0.2
1301.5	−4	4	−4	1	0.0
1386.7	−3	3	−3	2	0.1
1398.5	−4	3	−4	1	−0.1
1420.5	−4	4	−4	2	0.0
1432.7	−5	4	−5	1	−0.1
1511.8	−4	3	−4	2	0.3
1529.2	−5	3	−5	1	0.0
1567.1	−5	4	−5	2	0.1
1587.8	−6	4	−6	1	0.0
1656.4	−5	3	−5	2	0.2
1681.5	−6	3	−6	1	−0.1
1740.5	−6	4	−6	2	−0.2
1771.8	−7	3	−7	1	−0.7
1826.1	−6	3	−6	2	−0.3
1861.5	−7	2	−7	1	−0.2
1949.1	−7	3	−7	2	−0.1
2027.1	−7	2	−7	2	−0.3
2077.5	−8	1	−8	1	−0.5
			σ polarization		
627.5	5	4	6	1	−0.2
640.5	6	4	7	2	−0.1
666.9	4	4	5	1	−0.4
710.9	3,6	4,3	4,7	1,2	
722.2	4	4	5	2	−0.3
745.5	4	3	5	1	−0.7
752.7	5,5	4,3	4,6	2,2	−0.7,−0.3
759.2	2	4	3	1	−0.3
769.8	3	4	4	2	−0.1
792.2	3	3	4	1	
798.2	4	3	5	2	−0.1
805.2	4	4	3	2	0.3
812.8	1	4	2	1	−0.3
822.5	2	4	3	2	0.1
843.1	2	3	3	1	−0.4
848.2	3	3	4	2	−0.1
862.8	3	4	2	2	0.2
873.1	0	4	1	1	−0.2
881.0	1,3	4,3	2,2	2,1	
899.1	1	3	2	1	−0.8
903.3	2	3	3	2	−0.1
919.7	1	4	0	1	0.2
927.4	2	4	1	2	0.2
940.4	−1	4	0	1	
946.3	3,0	3,4	2,1	2,2	0.8,0.3
963.2	1	3	2	2	
994.1	0	4	−1	1	−0.2
1000.4	1	4	0	2	0.6
1011.5	1	3	0	1	
1020.0	−1	4	0	2	−0.1
1031.6	−1,0	3,3	0,1	1,2	
1081.9	0	4	−1	2	
1088.2	1	3	0	2	
1102.6	−3,−2	4,4	−2,−1	1,2	
1108.6	−1	3	0	2	
1176.1	−1,−2	4,4	−2,−3	2,1	
1197.2	−3,−3	3,4	−2,−2	1,2	
1267.2	−1	3	−2	2	−0.1
1274.2	−2	3	−3	1	0.1
1284.3	−2	4	−3	2	0.4
1295.7	−4	3	−3	1	
1305.4	−4	4	−3	2	−0.9
1315.0	−5	4	−4	1	1.4
1376.0	−2	3	−3	2	0.0
1387.3	−3	3	−4	1	−0.1
1409.4	−5,−3	3,4	−4,−4	1,2	−0.3,0.2
1420.5	−4	4	−5	1	−0.3
1431.5	−5	4	−4	2	−0.1
1501.6	−3	3	−4	2	0.7
1518.2	−4	3	−5	1	0.1
1539.7	−6	3	−5	1	−0.5
1556.1	−4	4	−5	2	0.2
1576.0	−5	4	−6	1	0.2
1646.4	−4	3	−5	2	0.5
1671.0	−5	3	−6	1	0.2
1692.0	−7	2	−6	1	−0.3
1730.0	−5	4	−6	2	0.1
1760.8	−6	4	−7	1	−0.3
1816.3	−5	3	−6	2	0.2
1851.6	−6	3	−7	1	0.0
1939.5	−6	4	−7	2	0.2
2018.4	−6	3	−7	2	−0.2
2068.6	−7	2	−8	1	−0.4

[a]In gauss.

and were not fit upon.

$$\hat{H}_Z = (0)_g^{(S)}\beta H_0 \hat{S}_z - g_n \beta_n H_0 \hat{I}_z + (aa)_g^{(S)}\hat{S}_a \hat{H}_a + (bb)_g^{(S)}\hat{S}_b \hat{H}_b + (cc)_g^{(S)}\hat{S}_c \hat{H}_c - [(0)_g^{(N)}H_0 \hat{N}_z + (aa)_g^{(N)}\hat{N}_a \hat{H}_a + (bb)_g^{(N)}\hat{N}_b \hat{H}_b + (cc)_g^{(N)}\hat{N}_c \hat{H}_c]. \quad (3)$$

The first term in Eq. (3) is the isotropic electron spin Zeeman interaction; the second term is the analogue for the proton spin. The next three are the anisotropic electron Zeeman interaction, and the remaining terms are the Zeeman interaction arising from the rotationally induced magnetic moment interacting with the external magnetic field. The effects of this latter term should be negligible for the ±0.5 G accuracy of the observations. None of the constants in these terms were fit upon. The g tensor components were determined from the relationships[21]

$$g_{aa} = 2.0023 - \epsilon_{aa}/2A \text{ etc.} .$$

The various matrix elements were calculated using the method of spherical tensor operators. This method has been fully described elsewhere[14,19,22,23] and so will not be given further treatment here.

In Table II are listed some representative contribu-

TABLE II. Contributions of the various Hamiltonian terms to a typical matrix element (in MHz) at $H = 1000$ G.

H spin–rotation	0–1000
H dipole–dipole	2
H Fermi	97
H anisotropic	1
H electron Zeeman	1400
H nuclear Zeeman	2
H rotational Zeeman	~0.5

tions of the various Hamiltonian terms to the total energy. Quite naturally the isotropic electron Zeeman is found to be the largest, followed by the Fermi contact and the spin–rotation interactions. It must be remembered that the rotational energy contribution is accounted for by subtracting it from the laser frequency.

SPECTRUM PREDICTION

In order to assign and fit the observed spectrum, it is first necessary to synthesize a similar spectrum. The total Hamiltonian used to calculate the spectrum was that one described in Eqs. (2) and (3) with the omission of the rotational Zeeman term since its contribution is negligible.

Once the Hamiltonian is chosen, a process for setting up and indexing the Hamiltonian matrices is needed. The projection of the total angular momentum on the field axis is the sum of the individual components along the field axis, $M_F = M_N + M_S + M_I$. M_F is a good quantum number for indexing the matrices. For each possible value of M_F there is set up a 1×1, 3×3, or 4×4 Hamiltonian. matrix–the dimension being the number of possible values of M_N, M_S, and M_I which sum to give M_F. For several fields the matrices are calculated and then diagonalized and the eigenvalues and transformation matrix for each diagonalization saved. Frequency differences between the appropriate Zeeman sublevels of each rotational level are then calculated. The direction cosines between the two rotational levels are calculated and transformed to the proper basis by the appropriate transformation matrices formed from the eigenvectors.

In order to present the spectrum as a field swept spectrum, the energy levels and the direction cosine matrices were calculated at 11 values of the magnetic field. Then, given a fixed laser frequency, the magnetic field giving that frequency for a given transition is calculated. This was done by quadratic interpolation between the three magnetic fields which give frequencies closest to the laser line. The intensity is calculated by interpolating the direction cosine matrix elements quadratically to that field. The intensity is proportional to the square of the direction cosine element. The resultant fields and intensities can be displayed as stick plots of intensity vs field or as Lorentzian derivatives on the same axes. By using 11 values of the magnetic field covering the region of the spectrum, the interpolation errors are less than the experimental error of 0.5 G.

ASSIGNMENT

The first assignement which must be arrived at in the complete analysis of this spectrum is obviously the rotational transition to which the Zeeman components of the observed lines belong. As the magnetic field strengths used in this experiment are not inordinately large (2100 G), the rotational frequency must be near that of the laser (2.783 THz). Additionally, as the observed lines move to higher field with increasing frequency, the rotational frequency must be below that of the laser. Likewise, because of the phenomenon of moving to higher field with increasing laser frequency, it can be shown from the considerations of the allowed transitions and possible levels, that there are $8N'+3$ possible lines for the π polarization. Here N' is the lower of the two rotational levels. Replete with this information, we predicted several rotational transitions. The rotational transitions which fulfilled, at least nominally, the above criteria were the $10_{2,9} \leftarrow 9_{1,8}$, $9_{2,7} \leftarrow 8_{1,8}$, and $8_{2,6} \leftarrow 7_{1,7}$—all b-type transitions. After predicting LMR spectra of all these transitons from the best available data, it was found that the $8_{2,6} \leftarrow 7_{1,7}$ transition best fulfilled the above requirements—both with respect to the number of lines and the overall qualitative appearance.

After settling on this assignment, some 92 completely resolved lines from both polarizations were assigned. Lines which were not completely resolved were omitted due to the inherent inaccuracy in assigning their positions. After refinement of the parameters by least-square fitting (vide infra) of these lines, the predicted and observed spectra are compared in Figs. 1 and 2. That the assignments must be correct is obvious from the goodness of fit of fields and the excellent agreement in relative intensity in comparison with the observed. Figure 3 shows the Zeeman levels of the two rotational levels involved in this spectrum. The transition at 659.7 G is shown by an arrow connecting the two sublevels involved. This is the fourth line from the low field end of the π polarization spectrum (the third strong line).

FITTING

Several of the parameters were adjusted by least-square fitting the observed spectrum. Because the lines were measured to 0.5 G, the refined parameters are generally more accurate than those determined previously. In looking at contributions of the various Hamiltonian terms in Table I, one can feel reasonably certain that a good fit of the observed data should be effected by fitting on ϵ_{aa}, ϵ_{cc}, $(0)_I$, and ν_0. The other terms of the Hamiltonian (except for the rotational Zeeman terms) are included in the calculation of the energy levels for the fit, but were not refined in the fit either because their magnitude was so small as to preclude a meaningful fit with these data, or because the constants were already well determined.

A convential least-squares adjustment of the observed spectrum was to be carried out. The resonant field of each line thus is supposed to be a function of ϵ_{aa}, ϵ_{cc}, $(0)_I$, and ν_0. The derivatives of field position with respect to each parameter are needed. This is accomplished by calculating the derivative of the frequency with respect to each parameter and then making use of the implicit function theorem

$$\left(\frac{\partial H}{\partial \epsilon_{aa}}\right)_\nu = \left(\frac{-\partial \nu}{\partial \epsilon_{aa}}\right)_H \Big/ \left(\frac{\partial \nu}{\partial H}\right)_{\epsilon_{aa}} \text{ etc. }, \tag{4}$$

to transfer to the proper derivative for a field swept spectrum. The quantities $H_{obs} - H_{calc}$ were calculated by

$$H_{obs} - H_{calc} = (\nu_{calc} - \nu_{obs})/(\partial\nu/\partial H). \tag{5}$$

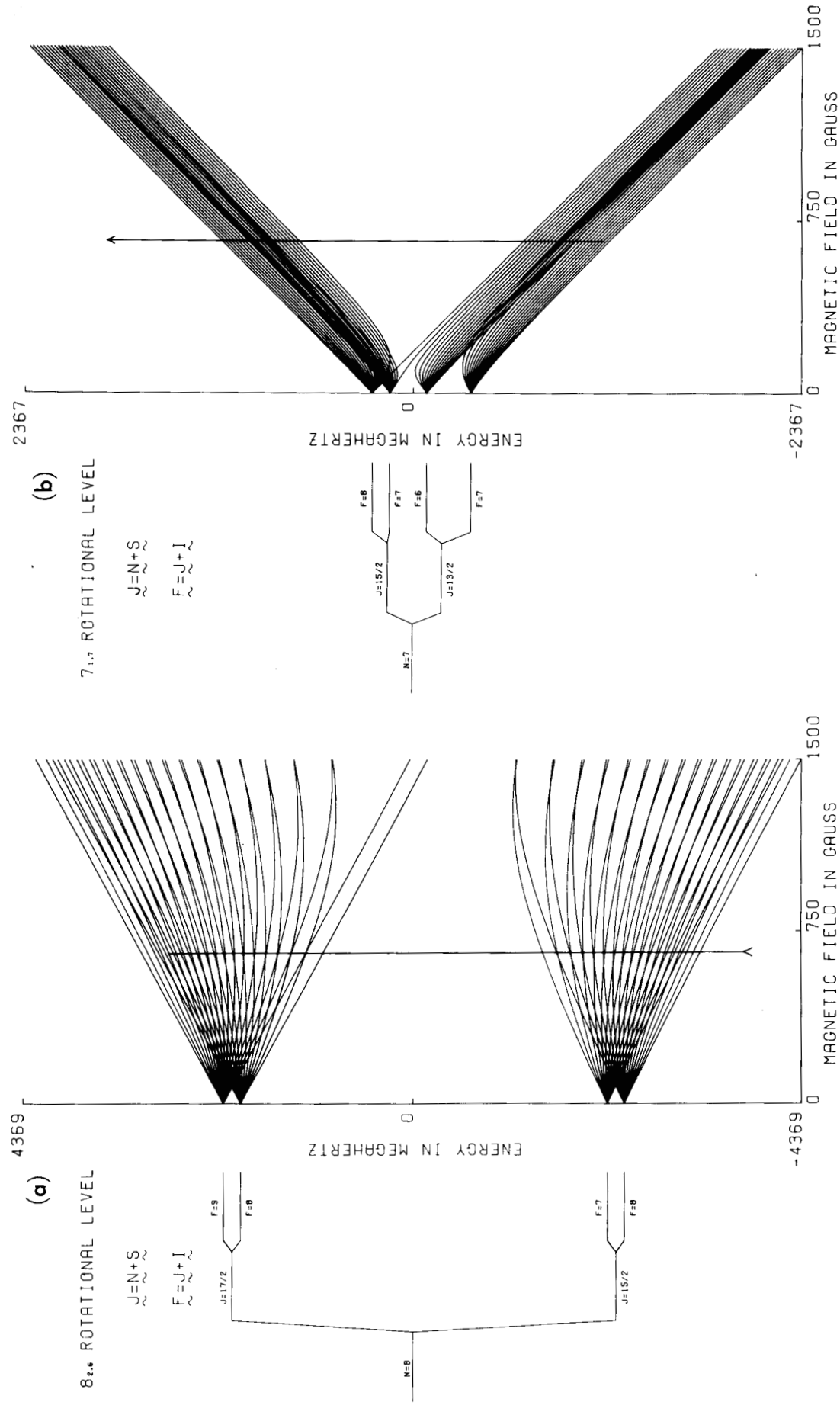

FIG. 3. This figure shows the Zeeman sublevels of each of the two rotational levels participating in these spectra. The zero-field splittings are shown to the left of each level. The $8_{2,6}$ (a) and the $7_{1,7}$ (b) have a solid line connecting the levels forming the line at 659.7 G in the π spectrum. This line is the fourth from the low field end in Fig. 1.

It was found that all four parameters were better determined by the data than by the initial guess. The estimated standard deviation of the observed field is given by

$$\left[\frac{\Sigma\{(H_{obs}-H_{calc})^2\}}{N_l-N_p}\right]^{1/2}=0.322\,\mathrm{G}, \qquad (6)$$

where N_l and N_p are the number of lines and number of parameters, respectively.

The results of the fitting are shown in Table III. Although ϵ_{aa} and ϵ_{cc} were fitted, the data actually determine the electronic spin–rotation splittings of the $7_{1,7}$ and $8_{2,6}$ levels, and these are the numbers listed in Table III. The constants used in calculating the spectrum, but which were not themselves fitted, are listed in Table IV.

From this analysis the four constants $(0)_I$, ν_0, $\Delta E(8_{2,6})$, and $\Delta E(7_{1,7})$ are obtained. The values are compared to the results of earlier work in Table III. The value of the Fermi contact constant, $(0)_I$, is very close to that obtained by Boland *et al.*[16] as is indicated in Table III. The values of the electron spin–rotation splitting for each state, $\Delta E(7_{1,7})$ and $\Delta E(8_{2,6})$, are reasonably close to those which can be calculated from the ϵ_{bb} and ϵ_{cc} constants of Boland *et al.*[16] and the K-dependent ϵ_{aa} found by Brown.[24] He obtained $\epsilon_{aa}(K=1)=11\,580$ MHz and $\epsilon_{aa}(K=2)=11\,430$ MHz.

The transition we have studied is the first b-type rotational transition observed for HCO. The best previous estimate of the A rotational constant was made by Brown and Ramsay[11] from an analysis of the optical spectrum. The effect of centrifugal distortion in HCO is quite large and the b-type rotational transition here reported gives the linear combination of A, Δ_{NK}, and Δ_K indicated in Table III when the values of B, C, Δ_N, δ_N, and δ_K found by Boland *et al.*[16] are inserted. If the value of Δ_{NK} of -0.92 MHz, which was obtained from a force field analysis by Mallinson,[25] is used, and the value of Δ_K of 707.5 MHz obtained by Brown and Ramsay by analysis of the optical spectrum is used, the value of A that results is 728.19 GHz. This compares closely with the A value of 728.32 GHz found by Brown and Ramsay.

TABLE III. Constants obtained from the current analysis and previous work.

Constants obtained from our analysis	Constants obtained from data of Brown[a] and Boland[b]
$\Delta E(7_{1,7})=333.5\pm6$[c]	$\Delta E(7_{1,7})=331.0$
$\Delta E(8_{2,6})=4329.1\pm9.5$[c]	$\Delta E(8_{2,6})=4326.5$
$(0)_I=389.7\pm1.3$[c]	$(0)_I=388.9$
$\nu_0=2779156.4$[d] ±2[c]	
Linear combination of A, Δ_{NK}, and Δ_K, determined by fit of LMR spectrum using the values of B, C, Δ_N, δ_N, and δ_K found by Boland[b]:	
$\nu_0\rightarrow A-76.91\,\Delta_{NK}-5\Delta_K=724821.6$	

[a] Reference 24.
[b] Reference 16.
[c] Two estimated standard deviations.
[d] Laser frequency used 2783066.6 MHz, Ref. 27.

TABLE IV. Constants used in fitting but not fitted themselves (in MHz).

$(0)_g^{(s)}=2.0009$	$(aa)_I=11.7$
β[a] $=1.39967$	$(bb)_I=3.8$
$g_n=5.585486$	$(cc)_I=-15.5$
β_n[a] $=7.623\times10^{-4}$	
$(aa)_g=-5.0208\times10^{-3}$	$(aa)_N=0.0$
$(bb)_g=1.7792\times10^{-3}$	$(bb)_N=0.0$
$(cc)_g=3.2416\times10^{-3}$	$(cc)_N=0.0$

[a] MHz/G.

Several additional LMR transitions of HCO have been observed by Radford.[26] The analysis of these transitions should yield other b-type rotational frequencies which, when combined with the other a-type transitions for HCO, should yield a complete set of rotational and centrifugal distortion constants for the molecule.

ACKNOWLEDGMENTS

This work was supported by grants from the Robert A. Welch Foundation and the National Science Foundation.

We would like to thank Dr. John Brown who was kind enough to provide us with preliminary results of his work on HCO.

[1] K. M. Evenson and M. Mizushima, Phys. Rev. A 6, 2197 (1972).
[2] R. F. Curl, Jr., K. M. Evenson, and J. S. Wells, J. Chem. Phys. 56, 5143 (1972).
[3] M. Mizushima, K. M. Evenson, and J. S. Wells, Phys. Rev. A 5, 2276 (1972).
[4] K. M. Evenson, J. S. Wells, and H. E. Radford, Phys. Rev. Lett. 25, 199 (1970).
[5] K. M. Evenson, H. E. Radford, and M. Moran, Appl. Phys. Lett. 18, 426 (1971).
[6] H. E. Radford, K. M. Evenson, and C. J. Howard, J. Chem. Phys. 60, 3178 (1974).
[7] P. B. Davies, D. K. Russell, B. A. Thrush, and F. D. Wayne, J. Chem. Phys. 62, 3739 (1975).
[8] C. J. Howard and K. M. Evenson, J. Chem. Phys. 61, 1943 (1974).
[9] G. Herzberg and D. A. Ramsay, Proc. R. Soc. London Ser. A 233, 34 (1955).
[10] J. W. C. Johns, S. H. Priddle, and D. A. Ramsay, Discuss. Faraday Soc. 35, 90 (1963).
[11] J. M. Brown and D. A. Ramsay, "Axis-Switching in the A^2A-X^2A Transition of HCO: Determination of Molecular Geometry," Can. J. Phys. (to be published).
[12] F. J. Adrian, E. L. Cochran, and V. A. Bowers, J. Chem. Phys. 36, 1661 (1962).
[13] R. W. Holmberg, J. Chem. Phys. 51, 3255 (1969).
[14] I. C. Bowater, J. M. Brown, and A. Carrington, J. Chem. Phys. 54, 4957 (1971), Proc. R. Soc. London Ser A 333, 265 (1973).
[15] J. A. Austin, D. H. Levy, C. A. Gottlieb, and H. E. Radford, J. Chem. Phys. 60, 207 (1974).
[16] B. J. Boland, J. M. Brown, and A. Carrington, "A Microwave Determination of some Molecular Parameters for HCO,"

Mol. Phys. (to be published).
[17]S. Saito, Astrophys. J. 178, L95 (1972).
[18]C. C. Lin, Phys. Rev. 116, 903 (1959).
[19]R. F. Curl and J. L. Kinsey, J. Chem. Phys. 35, 1758 (1961).
[20]W. M. Tolles, J. L. Kinsey, R. F. Curl, and R. F. Heidelberg, J. Chem. Phys. 37, 927 (1962).
[21]R. F. Curl, Mol. Phys. 9, 585 (1965).
[22]A. R. Edmonds, *Angular Momentum in Quantum Mechanics* (Princeton University, Princeton, 1960).
[23]D. M. Brink and G. R. Satchler, *Angular Momentum* (Clarendon, Oxford, 1968).
[24]J. Brown (private communication).
[25]P. D. Mallinson (private communication).
[26]H. E. Radford (private communication).
[27]F. R. Petersen, K. M. Evenson, D. A. Jennings, J. S. Wells, K. Goto, and J. J. Jimenez, IEEE J. Quantum Electron. QE11, 838 (1975).